Available online at www.sciencedirect.com

ScienceDirect

Procedia Materials Science 5 (2014) 154 – 163

Procedia Materials Science

www.elsevier.com/locate/procedia

International Conference on Advances in Manufacturing and Materials Engineering, AMME 2014

Magneto-mechanical coupled magnetostriction model for Terfenol-D actuator under step input

Raghavendra Joshi [a,*] Ravikiran Kadoli[a]

[a] *Department of Mechanical Engineering, National Institute of Technology Karnataka, Surathkal- 575025, India.*

Abstract

This paper discusses the design and magnetic circuit optimization of a Terfenol-D actuator. Optimization of the coaxial coils is being carried out for axial magnetic field based on shape factor. Experimental set up for measuring magnetic flux density and displacement of a Terfenol-D actuator are outlined. Numerical magnetic flux density of coaxial coils in free air are analyzed using Maxwell 2D solver. Experiments are conducted on a Terfenol-D actuator to measure the output displacement for different preloads under step input conditions. Magnetic field strength considering inductance of driving coils, magnetization using Jiles-Atherton model and magnetostriction using magneto-mechanical coupled magnetostriction model are evaluated to study the response characteristics of a Terfenol-D actuator. The results obtained from magneto-mechanical coupled magnetostriction model are verified with the experimental data.

Selection and peer-review under responsibility of Organizing Committee of AMME 2014

Keywords: Optimization, Terfenol-D actuator, Coaxial coils, Shape factor, Magnetic flux density, Maxwell 2D solver, Inductance, Jiles-Atherton model, Magnetostriction.

1. Introduction

Magnetostrictive material is a functional material with high displacement resolution, high force and fast response. Moreover, bi-directional transduction effects makes it more suitable for various applications (Liyi et al., 2011).

* Corresponding author. Tel.: +91 94812 19313
E-mail address: achyut61@gmail.com

Selection and peer-review under responsibility of Organizing Committee of AMME 2014
doi:10.1016/j.mspro.2014.07.253

Virtuous coupling exhibits between the mechanical and magnetic state of a magnetostrictive material. This material deforms when exposed to magnetic fields and changes its magnetization when stressed through this coupling. This material is commercially known as Terfenol-D and an alloy of Terbium, Dysprosium and ferrous material. Actuators using Terfenol-D are widely used in precision positioning, ultrasonics, active vibration control (Nakano, 2002; Zhang et al., 2004), DoD ink jet printer for droplet formation (Yoo and Park, 2010), and cutting tools for machining applications using Galfenol material, a class of magnetostrictive material (Atulasimha and Flatau, 2005). An extensive research work has been conducted on the output force characteristics, magnetostriction and actuators using Terfenol-D for many systems (Engdahl, 2000). However, the relationship between the magnetization and output strain of a Terfenol-D actuator exhibits strong hysteresis (Karunanidhi and Perumal, 2010). A complex ferromagnetic and elastic behaviour cannot be described by a simple linear model in various magnetostrictive materials. This behaviour has been shown as a coupled result of magnetic field, applied stress and load (Calkins et al., 2000; Zhou et al., 2007). In all these studies, emphasize is made to understand the behaviour of a Terfenol-D material using different analytical models to predict magnetostriction and its performance as well to use in few different applications. The present work outlines the design a prototype actuator driven with Terfenol-D material (symbolically represented by $Tb_{0.3}Dy_{0.7}Fe_{1.95}$) for automotive application. Based on shape factor of coil, the optimization of coaxial coils is carried out for axial magnetic field using analytical approach. An insight in to flux distribution is studied for coaxial coils in free air using Maxwell 2D solver. Experiments are being conducted on a Terfenol-D actuator to measure the output displacement for step input under different preload conditions. Magnetization and magnetostriction response of a Terfenol-D actuator model for step input under different pre-stress conditions are evaluated and results are compared with existing magnetostriction models as well with experimental data.

2. Structure and layout of a Terfenol-D actuator

The schematic layout of a Terfenol-D actuator is shown in Fig. 1 (a). In the present work, two coaxial coils namely coil 1 and coil 2 are chosen instead of coil and permanent magnet in the layout of a Terfenol-D actuator. The coil 1 is used to obtain bias magnetic field. It will enable the operation of the Terfenol-D actuator away from the initial non-linear portion of the magnetization curve. The magnetic field strength provided by coil 2 is superimposed with magnetic field from coil 1.

(a) (b)

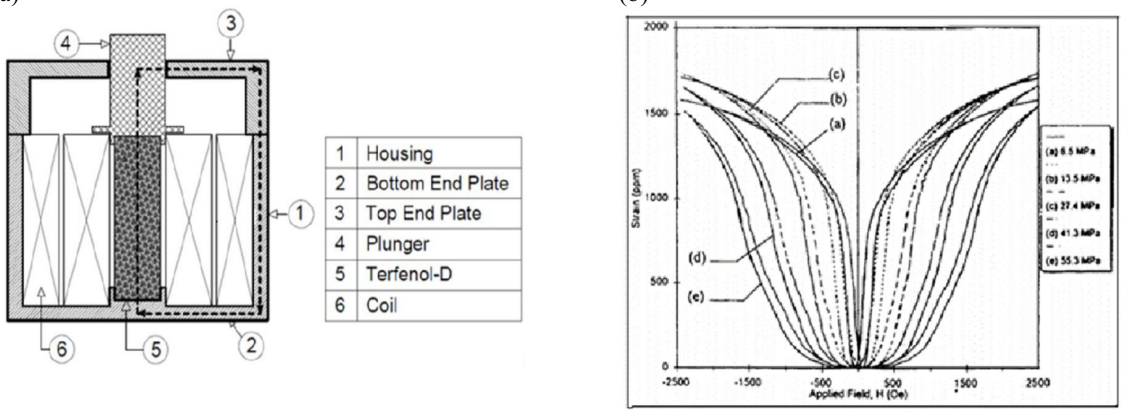

Figure 1. (a) Schematic layout of a Terfenol-D actuator (b) Magnetostriction curves of a Terfenol-D material against the applied magnetic field for different pre-stresses (Engdahl, 2000).

2.1 Coil design

Terfenol-D will be placed at the center of hollow cross sectioned co-axial coils. This arrangement is as good as conductor carrying current and Ampere's law is used to find the number of turns required for coils with suitable

wire diameter. Magnetostriction curves shown in Fig. 1(b) are referred, to determine the required magnetic field strength from the coils based on magnetostriction under an optimum prestress of 6.9 MPa (Engdahl, 2000). The magnetostrictive strain is 1000 to 1800 ppm for the applied field in the range of 550 Oe to 620 Oe i.e. approximately 48 kA/m to 52 kA/m in order to operate the actuator for linear behaviour. 17 SWG wire (BS6722, 1986) with a diameter of 1.423 mm and maximum amperage of wire as 4 A are chosen. The number of turns for coil 1 and coil 2 are 560 and 440 respectively to produce a magnetic field of 28 kA/m and 22 kA/m for 4 A input supply. Some of electrical parameters related to electrical aspects such as geometry of the coil and flux leakage, Q value of driving coil, magnetic coupling coefficient of the coil and inductance of the coil (Engdhal, 2000) are considered in the design of Terfenol-D actuator other than the number of coil turns and wire diameter. The details of parameters computed in electrical design are listed in Table 1.

Table 1. Details of parameters in electrical design

Parameter	Coil 1	Coil 2	Parameter	Coil 1	Coil 2
Magnetic coupling coefficient (K_c)	0.518	0.2684	Flux leakage of coil	8 %	12 %
Field factor $F(\alpha,\beta)$	1.02055	0.1791	Q value of coil	343729	91274
Power losses in a coil (P_{coil})	11.17	21.344	Inductance of coil (L)	3.878 mH	2.1824 mH
Magnetic field strength (H_{coil})	27 kA/m	21.2 kA/m	Resistivity of coil (R_{coil})	0.698 Ω	1.334 Ω
Inductance of Terfenol-D rod (L_{rod})	16.45 mH	18.3 mH	----	----	----

3. Magnetic circuit optimization of a Terfenol-D actuator

The magnetic circuit consists of a coaxial coils to provide magnetic field with Terfenol-D at its core, housing with other accessories like top and bottom end cover plate possessing magnetic resistance. The objective of the optimization is to improve the magnetic flux by minimizing the total magnetic resistance of the magnetic circuit of a Terfenol-D actuator. Soft magnetic material for housing, top and bottom end cover plate are chosen in an actuator assembly. Therefore the geometric parameters such as radii and length of coaxial coils are to be determined in the process of optimization. Considering the coil losses, the magnetic field at the center of hollow coil (Engdahl, 2000 and 2002) is given by,

$$H_{coil} = G_{coil} N_{coil} I \sqrt{\frac{2\pi}{l_T a_1} \times \frac{(\alpha+1)}{(\alpha-1)}} \tag{1}$$

In the above expression, the Fabry factor is introduced $G(\alpha,\beta)$ as,

$$G(\alpha,\beta) = \frac{1}{5}\left[\frac{2\pi\beta}{\alpha^2-1}\right]^{1/2} \ell n\left[\frac{\alpha+\sqrt{\alpha^2+\beta^2}}{1+\sqrt{1+\beta^2}}\right] \tag{2}$$

$\alpha = a_2/a_1$ and $\beta = l_T/2a_1$, Where a_1 and a_2 is the inner and outer radii of coil, N_{coil} is the number of coil turns, I is the input current to the coil and l_T is the length of the Terfenol-D rod.

The magnetic field declines rapidly towards the ends of the coil (Wang et al., 2006). Therefore the length of the coils should be slightly larger than the length of the Terfenol-D rod. The length of coaxial coils was assumed as 83 mm. With a view to reduce the magnetic leakage, the inner radius of the coil 1 was chosen close to the radius of the Terfenol-D rod. The inner radius of the coil 2 should be approximately equal to the outer radius of coil 1. The radius of the Terfenol-D rod was chosen to be 14 mm. With this the length and inside radii of the coils are fixed, the

objective will be to determine the optimum values of outer radii of coils. The analytical treatment discussed in Dehui et al., (2008) is adopted to optimize the outside radii of coils. The coil design will be based on an optimized value of the shape of the coil and cross-sectional area of the coil as follows,

$$\left\{ \text{Max}\, G_{coil}(\alpha,\beta);\ \frac{K_{coil} H_{coil} l_T}{4\times10^{-6}} \le \text{A}_{coil} \le \frac{K_{coil} H_{coil}\ l_T}{2\times10^{-6}} \right\} \tag{3}$$

The maximum fabry factor G_{coil} for coil 1 is 0.16349 with $\alpha = 2.2121$, $\beta = 2.5151$ and for coil 2 is 0.14425 with $\alpha = 1.5333$, $\beta = 1.1067$ indicates the geometry of coaxial coils, in which the magnetic field produced by them are for the least dissipated resistive power (Engdahl, 2000). The details of coaxial coils are listed in Table 2.

Table 2. Details of coils

Parameters	Coil 1	Coil 2
Shape factor (G_{coil})	0.16349	0.14425
Coil compensation coefficient (K_{coil})	0.981	1.233
Area of coil (A_{coil})	7.47×10^{-4} m^2	5.81×10^{-4} m^2
Current density (J)	1350 kA/m^2	1060 kA/m^2
Inner and outer radii $(a_1$ and $a_2)$	16.5 mm and 36.5 mm	37.5 mm and 57.5 mm
Length of coil (l_{coil})	83 mm	83 mm

4. Experimental setup for measuring magnetic flux density

The experimental arrangement for measuring magnetic flux density is shown in Fig. 2 (a). Magnetic flux density has been measured using Lakeshore guassmeter-410 with hall probes HT5891 (Transverse Probe) and HA3863 (Axial Probe). Transverse probe has a hall sensor mounted parallel to the probe axis and measures magnetic fields perpendicular to the probe axis. Axial probe has a hall sensor mounted perpendicular to the probe axis and measures magnetic fields parallel to the probe axis. APLAB-LD6405 power supply is used for varying step input to coils from 0 A to 4 A in a step of 0.25 A. The distance between the coils and the probe is maintained constant 5 mm for better measurement.

a

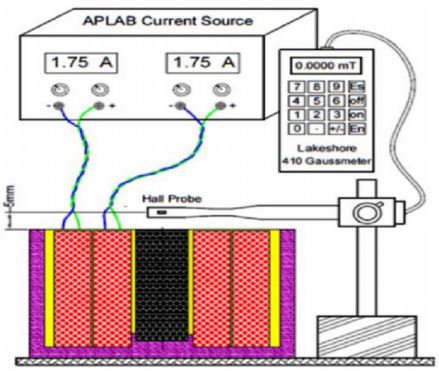

b

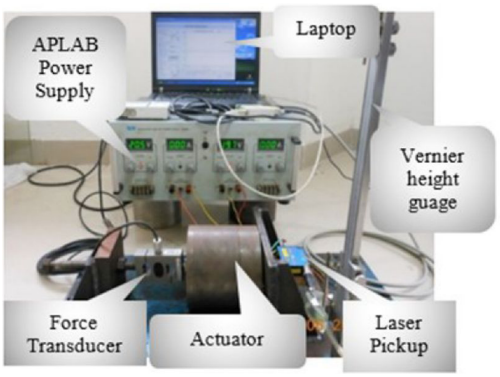

Fig. 2. Experimental setup for measuring (a) magnetic flux denstiy (b) displacement of a Terfenol-D actuator.

5. Experimental set up for measuring displacement of a Terfenol-D actuator

The experimental setup shown in Fig. 2 (b) consists of actuator assembly, pre-stress mechanism consists of accessories like Belleville springs, force transducer and laser pickup held on to digital vernier height guage and APLAB power unit to supply a step input up to 4 A. Belleville springs are used to preload the Terfenol-D rod. Force transducer make HBM S2 is used for measuring applied preload. It is interfaced to computer through Lab VIEW environment which will make use of NI 9237 to give an output in the form of graphical display for the force being applied on Terfenol-D rod. Laser pickup sensor is used for measuring the displacement of Terfenol-D. The measuring range of laser pickup is 10 mm and is held in a vernier height for positioning laser pickup to the measuring end. The best measuring range for the laser pickup is between 24 to 28mm. Laser pickup is interfaced to computer via USB converter RS 422. The numerical data is obtained using ILD 1402 measurement tool software (ILD 1402 Tool V2.03). It will graphically display the output and as well the output is stored in excel format.

6. Analytical magneto-mechanical coupled magnetostriction model for Terfenol-D actuator

Conventionally it is very difficult to understand the constitutive behaviour of Terfenol-D through modelling. The presence of large magnetostriction anisotropy, low magneto- crystalline anisotropy and a twinned dendritic structure gives rise to complex domain level processes which are not completely understood (Huang and Jin, 2008). The Jiles-Atherton model (Jiles and Atherton, 1986) quantifies the total magnetization of a ferromagnetic material as sum of an irreversible component due to domain wall motion and a reversible component due to domain wall bowing. In the present work Jiles-Atherton hysteresis model, and analytical magnetostriction model is used to study various performance parameters of the actuator.

6.1. The field intensity from the drive coils of a Terfenol-D actuator

Magnetic field intensity H induced in a Terfenol-D rod for an applied step input to coil can be expressed as:

$$H = \frac{B_T}{\mu^\sigma} \tag{4}$$

Where B_T is a magnetic flux density and μ^σ is the relative magnetic permeability at constant stress of a Terfenol-D.

Further the inductance of driving coils is considered for computing the distribution of magnetic field intensity on Terfenol-D rod. The inductance L of coil is a function of input current and applied pre-stress has been used to express the maximum magnetic flux density on Terfenol-D rod (Liyi et al., 2011).

$$B_T = L.I/N.A_T \tag{5}$$

When the actuator coil is excited with step input, the magnetic field strength varies exponentially as follows.

$$H = \frac{L_1.I_1\left[1-e^{-\frac{tR_1}{L_1}}\right]}{N_1 A_T\ \mu^\sigma} + \frac{L_2.I_2\left[1-e^{-\frac{tR_2}{L_2}}\right]}{N_2\ A_T\ \mu^\sigma} \tag{6}$$

The inductance L_1 and L_2 are inductances of coil 1 and coil 2 which is resultant of self-inductance (Engdahl, 2002) and mutual inductance (Young et al., 2007). Shape factor of the coil also governs the inductance (Engdahl, 2000 and Grunwald and Olabi, 2008). I_1 and I_2 are applied step input to coil 1 and coil 2 , and A_T is the cross-sectional area of a Terfenol-D rod.

6.2. Evaluation of magnetization using Jiles-Atherton model

The total magnetization is composed of reversible magnetization and irreversible magnetization. The J-A model of hysteresis starts with anhysteretic magnetization in which coupling of field and inter domain magnetization are formulated using mean field theory.

$$M_{an}\left(H_{eff}\right) = M_s\left(\coth\left(H_{eff}/a\right) - \left(a/H_{eff}\right)\right) \tag{7}$$

Where M_s is the saturation magnetization, a is the shape parameter of anhysteretic curve and H_{eff} is the effective magnetic field.

$$H_{eff} = H + \alpha M \tag{8}$$

Where H is the applied magnetic field can be computed using Eq. (6), M is the magnetization and α is the interdomain coupling.
The irreversible magnetization depends on magnetic field is described by the governing equation as:

$$\frac{dM_{irr}}{dH} = \frac{M_{an} - M_{irr}}{k\delta - \alpha\left(M_{an} - M_{irr}\right)} \tag{9}$$

Where k is a domain wall pinning constant and parameter δ is +1 when $dH/dt > 0$ and -1 when $dH/dt < 0$.
Reversibility coefficient c allows the reversible magnetization of the material to be written in terms of irreversible magnetization and anhysteretic magnetization as:

$$M_{rev} = c\left(M_{an} - M_{irr}\right) \tag{10}$$

The total magnetization is then dictated by the superposition of the irreversible and reversible magnetization and is given as:

$$M = M_{\text{rev}} + M_{\text{irr}} \tag{11}$$

6.3. Magneto-mechanical magnetostriction model

An extensive work has been reported by many researchers to improve the magnetostrictive model by accounting various influencing parameters like magnetization, applied pre-stress and Young's modulus. One of the characteristic property of Terfenol-D material is that the mechanical strain will occur if it is subjected to a magnetic field, applied stress both individually or combined. The dependencies can be represented by the piezomagnetic equation given by Eq. (12).

$$\lambda = \frac{\sigma}{E^H} + d_{33}H \tag{12}$$

Where λ is the magnetostriction, σ is the applied stress, E^H is the young's modulus at constant magnetic field, H is the magnetic field intensity and d_{33} is the dynamic strain coefficient.
The magnetostriction given by Eq. (12) can be expressed by substituting the magnetic field as a function of magnetization (Karunanidhi and Singaperumal, 2010),

$$\lambda = \frac{\sigma}{E_H} + \frac{d_{33} M}{\left(\mu^T - 1\right)} \tag{13}$$

Assuming the pre-stress is sufficiently large, magnetostriction can be approximately represented as a single valued function of magnetization (Calkins et al., 2000) as:

$$\lambda = \frac{3}{2} \frac{\lambda_s}{M_s^2} M^2 \tag{14}$$

Accounting the effect of pre-stress σ as well as ΔE effect, magnetostriction represented (Zheng and Liu, 2005) as follows:

$$\lambda = \frac{\sigma}{E_s} + \frac{\lambda_s}{2} \tanh\left(\frac{2\sigma}{\sigma_s}\right) + \left(1 - \frac{1}{2} \tanh\frac{2\sigma}{\sigma_s}\right) \lambda_s \left(\frac{M}{M_s}\right)^2 \tag{15}$$

Where σ_s is the saturation prestress, M_s is the saturation magnetization and λ_s is the saturation magnetostriction.

7. Results and discussion

Magnetic flux density of coaxial coils in free air along the axial and radial direction are analyzed using Maxwell 2D solver based on the procedure outlined in Brauer (2006). Response characteristics such as output displacement of a Terfenol-D actuator for step input under different preload conditions are discussed. Model response curves are evaluated using magneto-mechanical coupled magnetostriction model and the same have been verified with experimental results**.**

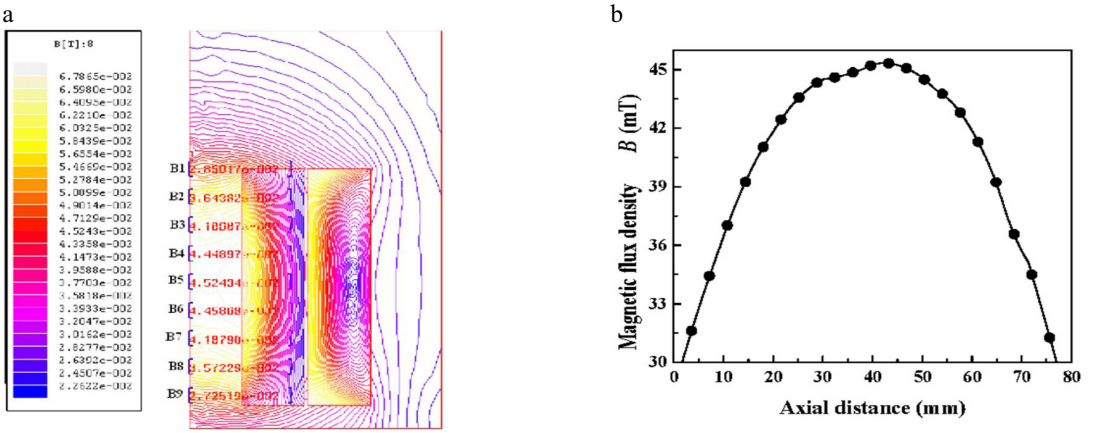

Fig. 3 (a) Coaxial coils with points along axial direction in a Maxwell 2D solver (b) Axial flux density distribution along the center line of coaxial coils in free air.

7.1 Numerical magnetic flux density for co-axial coils in free air

The axial magnetic flux density has been measured at specified points with coaxially placed coils alone for step input of 4 A. Maximum magnetic flux density has been observed at the centre and gradually decreases on either side from the centre of Terfenol-D rod. It is also observed that the magnitude of magnetic flux density is almost the same for the corresponding points on either side from the centre of Terfenol-D as shown in Fig. 3 (a) and (b). The magnetic flux density along the radial direction at each specified point has been measured by varying the step input

from 0 to 4 A with a step of 0.25 A. It has been observed that the magnitudes of magnetic flux density along the radial direction is gradually decreasing with increasing distance from the Terfenol-D rod as shown in Fig. 4 (a) and (b).This is because the magneto motive force generated by the coaxial coils is goes on decreasing as the distance increases from Terfenol-D. The points B_1 and B_2 created are very close and nearer to Terfenol-D compared to B_3 and B_4, due to which magnetic flux density is almost same has been observed.

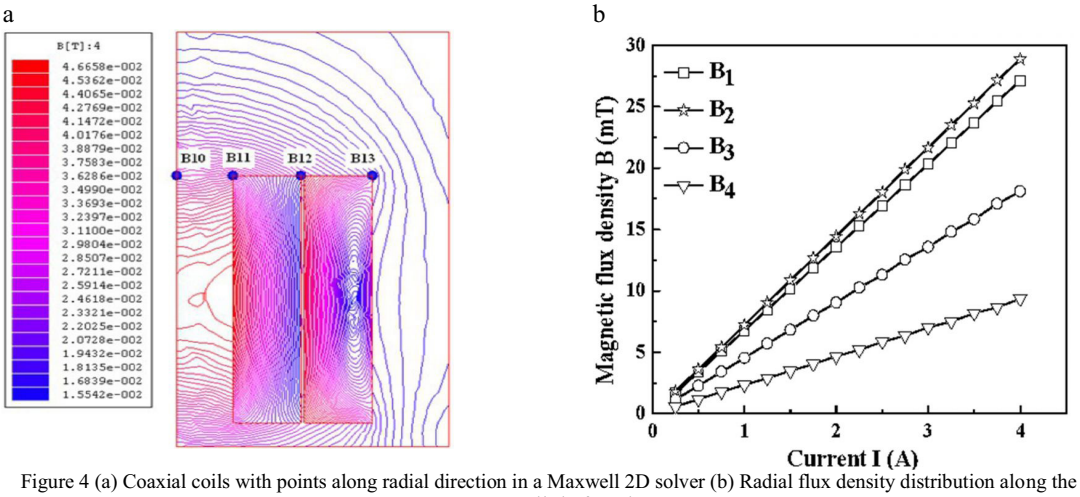

Figure 4 (a) Coaxial coils with points along radial direction in a Maxwell 2D solver (b) Radial flux density distribution along the coaxial coils in free air.

7.2 Magnetostrictive model response curves

The magnetization and magnetostriction responses for a Terfenol-D actuator for zero preload are discussed using theoretical model. Theoretically the magneto-mechanical characteristics like magnetic field using Eq. (6) , magnetization using Eq. (11) , magnetostriction using Eq. (13), (14) and (15) are computed as a function of time.

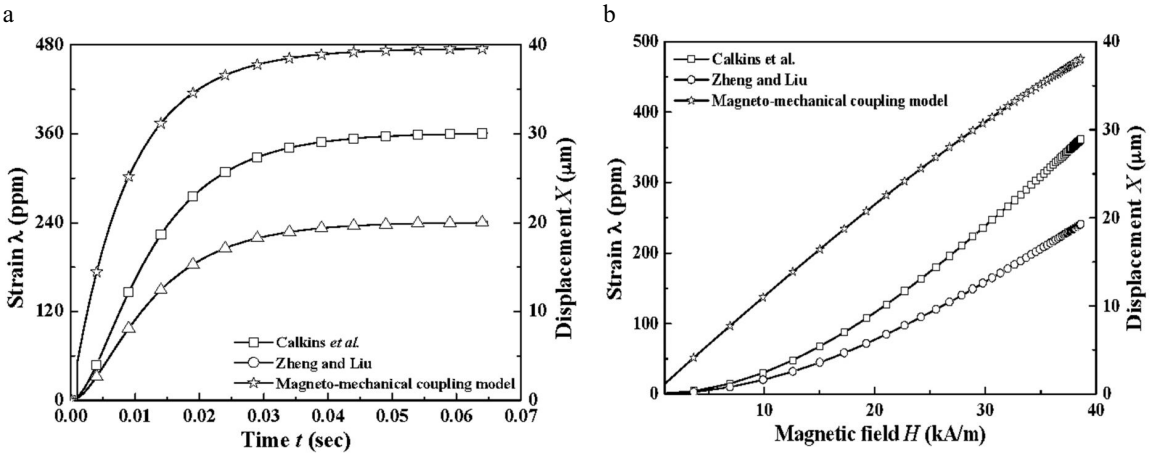

Fig. 5 (a) Comparison of strain and displacement with (a) magneto-mechanical model (b) quadratic model as a function of time.

The minimum and maximum strain obtained are 51 and 475 ppm for a step input of 0.25 A and 4 A respectively from Fig. 5 (a). It is also observed that the time required for the response to reach from the point of excitation to steady state point is constant as the input increases and equal to 171 ms from Fig. 5 (a). Fig. 5 (b) shows the comparison of strain obtained with different magnetostriction models against the time. The output strain obtained with magneto-mechanical model compared to models reported by Calkins et al. (2000) and Zheng and Liu (2005) is

also almost linear for an applied input i.e. strain is proportional to the applied input. Percentage in strain of 24 and 50 % increase is obtained with magneto-mechanical model when compared to Calkins et al., (2000) and Zheng and Liu (2005) models.

7.3. Experimental response curves of a Terfenol-D actuator under different preload conditions

Experiments are conducted to measure the displacement of a Terfenol-D actuator under different preloading conditions. The experimental operating conditions are varying dc input simultaneously to coil 1 and coil 2, constant biasing field to coil 1 and varying dc input to coil 2 and varying biasing field to coil 1and constant dc input to coil 2. The experiment was conducted for one completer cycle i.e. increasing and decreasing input and the data was collected at a frequency of 1 kHz. Fig. 6 (a) shows the strain induced in a Terfenol-D actuator by varying the step input to coaxial coils. The step input is increased from 0 to 4 A and again decreased to 0 A in steps of 0.25 A equally to coaxial coils of a Terfenol-D actuator. The maximum strain of 373 ppm at an applied step input of 4 A. The strain obtained by varying biasing to coil 1 is more than the strain obtained by varying step input to both coils as the net available magnetic field produced by the coaxial coils is more at each excitation. On the other hand strain achieved is less by varying biasing field to coil 1 when compared to strain achieved with constant biasing to coil 1. It is because, coil 2 is having less number of turns compared to coil 1 and it is also far away from Terfenol-D in the actuator assembly due to which the magneto motive force generated by the coil 2 may not reach effectively to the measuring end of Terfenol-D rod to achieve more strain though the net available magnetic field is same in both cases. It has been summarized that by biasing the magnetic field improves the performance of Terfenol-D actuator.

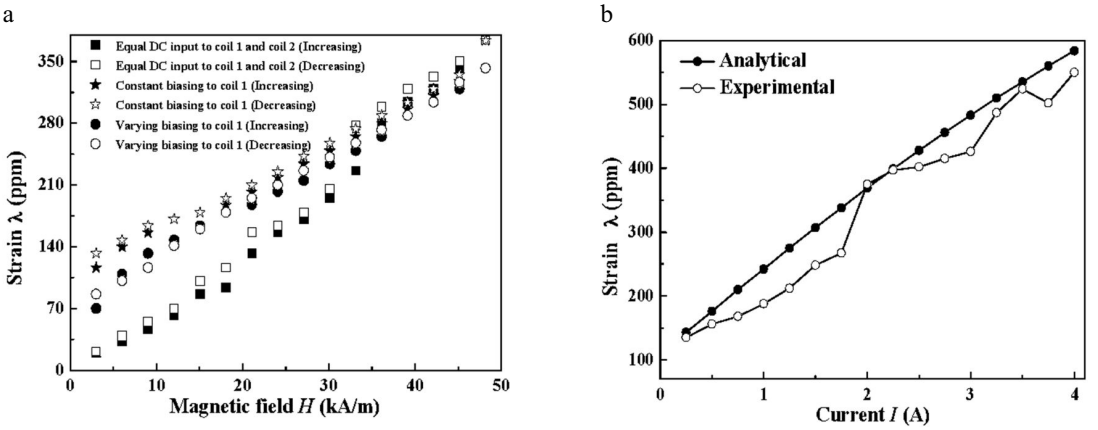

Fig. 6 (a) Strain under different operating conditions (b) Analytical and experimental strain comparison of a Terfenol-D actuator.

7.4 Prediction of Terfenol-D actuator strain under 2000 N preload: Analytical and Experimental

Fig. 6 (b) shows the comparison of strain obtained from experiment and magneto-mechanical magnetostriction model for a preload of 2000 N. Maximum strain obtained is 584 ppm with the magneto-mechanical model and 550 ppm from experimental at an applied input of 4 A. The deviation of 10 % in strain from experiment has been observed when compared to magnetostriction model output for 2000 N preload. This may be due to ohmic losses, source instability such as resistance of a coil and air gap present in an actuator among different components due to which there would be flux leakage, are few reasons for the deviation.

8. Conclusions

A Prototype Terfenol-D actuator has been designed and fabricated for automotive applications. Based on shape factor of coil, the optimization being carried out was effective to achieve magnetic field from the drive coils. Maximum magnetic flux density has been observed at the center and gradually decreases on either side from the

center from the axial distribution of coaxial coils. On the other hand, the magnitude of magnetic flux density is gradually decreasing when moving away from the center along the radial direction of coaxial coils. From the experiments, the maximum strain of 373 ppm for a step input of 4 A to coils has been observed. Constant or varying a biasing field to coil 1 has improved the performance of a Terfenol-D actuator compared to supply of equal input to coaxial coils. Response time of a Terfenol-D actuator was 171 ms from the magnetostrictive model.

Acknowledgements

The research activity reported here was funded by the Ministry of Human Resource and Development (MHRD) R and D projects (No.26-11/2004- TS V, Dated 31-03-05), New Delhi, India. The authors would like to acknowledge the contribution of Mr. Sreekanth Thota, PG student of 2006, NITK, Surathkal for inputs related to hysteresis modelling employed here and DMRL, Hyderabad for providing Terfenol-D rod.

References

Atulasimha, J. Flatau, A.B., 2005. Energy-based constitutive model for magnetostrictive materials and its application to Iron-Gallium alloys. MRS online proceedings Library, 888.

Brauer, J. R., 2006. *Magnetic actuators and sensors*. A John Wiley & Sons Inc., Publication, Hoboken, New Jersey.

BS6722, 1986. *Recommendations for dimensions of ferrous & non-ferrous metallic materials in wire form*. British Standards Institution, ISBN: 0 580 15358 4.

Calkins, F.T., Smith, R.C., Flatau, A. B., 2000. Energy-Based Hysteresis Model for Magnetostrictive Transducers. IEEE Transactions on Magnetics 36, 429-439.

Dehui, L., Quanguo, L., Yuyun, Z., 2008. Magnetic circuit optimization design of Giant magnetostricitve actuator. 9th International Conference Computer-Aided Industrial and Conceptual Design, Kunming, 688-692.

Engdahl, G., 2000. *Handbook of Giant Magnetostrictive materials*. Royal Institute of Technology, Stockholm, Sweden.

Engdahl, G., 2002. Design procedure for optimal use of giant magnetostrictive material in magnetostrictive actuator applications. Actuator 2002, 8th International Conference on New actuator, Bremen, Germany, 554-557.

Grunwald, A., Olabi, A.G., 2008. Design of a magnetostrictive (MS) actuator. Sensors and Actuators A. 144, 161-175.

Huang, Y. Y., Jin, Y. M., 2008. Phase field modelling of magnetization processes in growth twinned Terfenol-D crystals. Applied Physics Letters 93 (14), 142504-3.

Jiles, D. C., Atherton, D. L., 1986. Theory of ferromagnetic hysteresis. Journal of Magnetism and Magnetic Materials 61, 48-60.

Karunanidhi, S., Singaperumal, M., 2009. Design, analysis and simulation of magnetostricitve actuator and its application to high dynamic servo valve. Sensors and Actuators 157, 185-197.

Liyi, L., Chengming, Z., Baiping, Y., Xiaopeng, L., 2011. Research of a Giant Magnetostrictive Valve with Internal Cooling Structure. IEEE Transactions on magnetics 47, 2897-2900.

Nakano, H., 2002. Angstrom positioning system using giant magnetostriction actuator for high power applications, Proceedings of IEEE. Hitachi, Ibaraki, Japan, 1102-1107.

Wang, L., Ye, H., Liu, Y. T., Yao, S. M., 2006. Analysis and optimization for uniformity of magnetic field during the giant magnetostriction, *Journal* of Physics 48, 1336-1340.

Yoo, J., Park, Y., 2010. Experimental investigation of magnetostrictive DoD inkjet head for droplet formation. Current Applied Physics 1-7.

Young, H. D., Freedman, R. A., Ford, L., 2007. *University physics with modern physics with mastering physics*. 12th Edition, Addison-Wesley Publishers.

Zhang, T., Jiang, C., Zhang, H. Xu, H., 2004. Giant magnetostrictive actuator for active vibration control. Smart Materials and Structures 13, 473-477.

Zheng, X.J., Liu, X.E., 2005. A nonlinear constitutive model for Terfenol-D rods. Journal of applied Physics 97(5), 1-8.

Zhou, H., Zhou, Y., Zheng, X., 2007. Active vibration control of Terfenol-D rod of giant magnetostrictive actuator with non-linear constitutive relations. Journal of Theoretical and Applied mechanics 45, 953-967.